Downloaded from SAE International by David Sims-Williams, Tuesday, April 21, 2015

SAE INTERNATIONAL

The Effects of Unsteady Flow Conditions on Vehicle in Cabin and External Noise Generation

2015-01-1555
Published 04/14/2015

Charalampos Kounenis, David Sims-Williams, Robert Dominy, and Arganthaël Berson
Durham University

Nicholas Oettle and Claire Freeman
Jaguar Land Rover

CITATION: Kounenis, C., Sims-Williams, D., Dominy, R., Berson, A. et al., "The Effects of Unsteady Flow Conditions on Vehicle in Cabin and External Noise Generation," SAE Technical Paper 2015-01-1555, 2015, doi:10.4271/2015-01-1555.

Copyright © 2015 SAE International

Abstract

A vehicle driving on the road experiences unsteady flow conditions which are not generally reproduced in the development environment. This paper investigates the potential importance of this difference to aeroacoustics and hence to occupant perception and proposes a methodology to enable better ranking of designs by taking account of wind noise modulation.

Two approaches of reproducing the effects of unsteady wind on aeroacoustics were investigated: an active wind tunnel Turbulence Generation System (TGS) and a quasi-steady approach based on measurements at a series of fixed yaw angles. A number of tools were used to investigate the onset flow and its impacts, including roof-mounted probe, acoustic heads and surface microphones. External noise measurements help to reveal the response of separate exterior noise sources to yaw.

The noise experienced by the driver or passenger ear facing the side-glass is dominated by increased sound pressure levels when the adjacent side-glass is the leeward side of the vehicle with some non-linear effects as leeward yaw produces first accelerated flow and then separation.

In part because of non-linearity in response to yaw, a challenging parameter for a wind tunnel simulation of dynamic yaw is achieving a wide enough variation in yaw angle and this work suggests that considering an appropriate range of yaw angles is more important than capturing the dynamics.

In terms of passenger perception, the most important effect of a time-varying onset flow was demonstrated to be the modulation of wind noise rather than the increase in time-averaged cabin noise. For the case considered, at 130 km/h, the impact of wind-noise modulation was found to be equivalent to an extra 1-2 dBA in terms of passenger perception, while the increment in time-averaged cabin noise would be only 0.2 dBA.

Introduction

On the road, a vehicle encounters an unsteady flow due to turbulence in the natural wind, the unsteady wakes from other road vehicles and the stationary wakes of roadside obstacles as a result of traversing through them [1]. This can be important from the point of view of vehicle handing ([2,3,4,5,6,7,8]), fuel economy ([9, 10]) or wind noise ([11,12,13,14,15,16]).

Since the 1980's, there has been a continued effort to minimize wind-induced noise in the passenger interior. At higher vehicle speeds typical of highway driving aerodynamic noise tends to dominate over other sources (e.g.: as discussed by [13, 17]) and aerodynamic noise has tended to grow in importance as other sources of noise have been better attenuated in modern vehicles. Various researchers including [18,19,20,21] discussed that broadband noise sources which normally dominate the passenger compartment are related to A-pillar vortex flow or separated flows on the side or rear of the vehicle. These usually occur at mid and high frequencies and, as dipole sources, they approximately scale with velocity to the power of 6 (e.g.: as discussed by [22]). Tonal noise sources (roof racks, antenna, etc.) are also a concern, but once identified and controlled, they are not the dominant noise sources. Vehicle aeroacoustic sources at low frequencies, such as the separated wake regions, are generally less important, except when linked to underfloor flows (e.g.: [23]).

Aeroacoustic wind tunnels allow repeatable, high-fidelity assessment of cabin noise and their measurements correlate well with on-road wind noise under low wind, low turbulence conditions. However, a vehicle driving on the road experiences unsteady flow conditions which are not generally reproduced in the development environment and the vehicle aerodynamic performance in windy conditions can be expected to have an important influence on customer perception.

This work seeks to move forward the understanding of how differences between the development and on-road environment can impact wind noise and to point the way to being able to better assess

Downloaded from SAE International by David Sims-Williams, Tuesday, April 21, 2015

a vehicle's aeroacoustic performance in windy conditions. In particular, the impact of noise modulation on perceived wind noise is considered alongside impacts on average noise level.

Experimental Method

Test Vehicle

A vehicle typical of a European luxury saloon was used throughout this study and has a nominal drag coefficient of $C_d = 0.29$ and a frontal area of $A_f = 2.33$ m^2 [24]. Body gaps were fully taped for all data presented in this paper in order to minimize measurement uncertainties linked to sealing. The engine bay intake and exterior vents were open (untaped) and the air-conditioning / ventilation was switched off. Finally the suspension was free and there was no ballast beyond the test equipment. An image of the test vehicle in the wind tunnel is shown in Figure 1.

Figure 1. Test vehicle in the wind tunnel test section.

Pininfarina Wind Tunnel

The wind tunnel investigation was carried out in the Pininfarina wind tunnel in Torino, Italy. The tunnel is of closed-return type with an open jet test section and its nozzle area is of 11 m^2 with a contraction ratio of 6.9:1 [18]. A cross-sectional view of the wind tunnel is shown in Figure 2. The tunnel allows for moving ground and/or rotating wheel measurements but the measurements presented are with stationary wheels and belt. The ambient noise in the test section has been progressively reduced with a reported test section (out-of-flow) background noise level of 68 dBA at 100 km/h. Facility details related to aeroacoustics are available in [18, 25, 26].

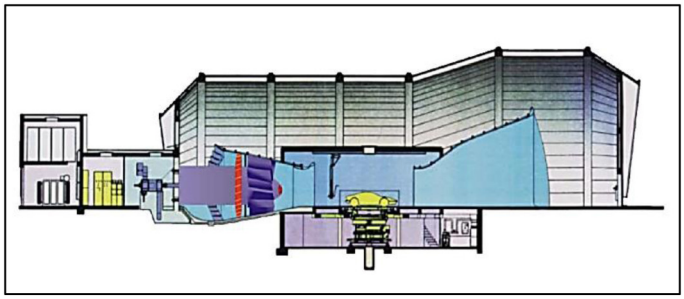

Figure 2. Cross-sectional view of Pininfarina wind tunnel layout [27].

This tunnel includes the capability to create elevated turbulence levels with relatively long length scales through a pioneering active "Turbulence Generation System" (TGS). While the reported free stream turbulence in standard condition (with an empty test section) is 0.26%, the TGS makes is possible to create turbulence intensities in the region of up to 6% with length scales of a few meters. This is achieved using a set of dynamic spires at the upstream end of the wind tunnel contraction (Figure 3). Two modes of operation were used for the work reported here (Table 1). The 4D1 dynamic yaw mode seeks to simulate an oscillating yaw angle through the opening of the TGS flaps in turn with a frequency of 1 Hz [14].

Table1. Description of the TGS modes used during wind tunnel testing.

TGS Mode	Description
5AL	Moderate Traffic (Random Mode)
4D1	1 Hz Dynamic Yaw

Figure 3. Pininfarina wind tunnel turbulence generation system [14].

Binaural Acoustic Head Measurements

The interior noise was measured using HEAD Acoustics HMS III acoustic heads. Each device contained two HDM I.0 digital artificial head microphones, each with a frequency response from 3 Hz to 20 kHz, a transmission error of ± 0.1 dB and nominal dynamic range of 118 dB [14]. Calibration factors (programmable in 10 dBSPL increments) were set according to the noise level for each measurement. Acoustic data were recorded at 48 kHz.

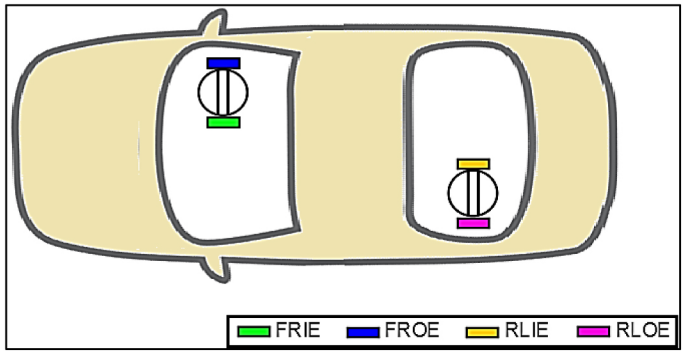

Figure 4. Acoustic head channel names and positions.

Downloaded from SAE International by David Sims-Williams, Tuesday, April 21, 2015

The test vehicle was right-hand drive. In the wind tunnel test, two heads were used, one on the front right (driver's) seat and one on the rear left seat. When presenting data collected using the acoustic heads, the data recorded by each ear channel is referred to by the channel name. The names of these channels are listed in Table 2 and corresponding positions are shown in Figure 4. The acronym used to differentiate each channel contains information on both the head position and ear microphone used.

Table 2. Acoustic head channel names.

Channel Name	Description
FRIE	Front Right Inner Ear
FROE	Front Right Outer Ear
RLOE	Rear Left Outer Ear
RLIE	Rear Left Inner Ear

Surface Microphone Measurements

Acoustic pressure fluctuations on the surface of the vehicle were recorded using B&K 4949 surface microphones. These microphones have a 5 Hz to 20 kHz frequency range and 30-140 dBSPL dynamic range. They have an external diameter of 10 mm and thickness of 2.5 mm and were surface-mounted using manufacturer-supplied 35 mm mounting pads and secured with tape. The wires were taped in such a way as to minimise the flow disturbance to microphones downstream [28].

A set of 16 microphones were repositioned between measurements to capture data at approximately 35 locations over the front right-hand sideglass and across the windshield. Figure 5 illustrates the locations on the sideglass and the flow structure (from [29]). The sorting of microphones into classifications was based on the SPL response to yaw (discussed later) with naming based on the location of the majority of microphones within each classification.

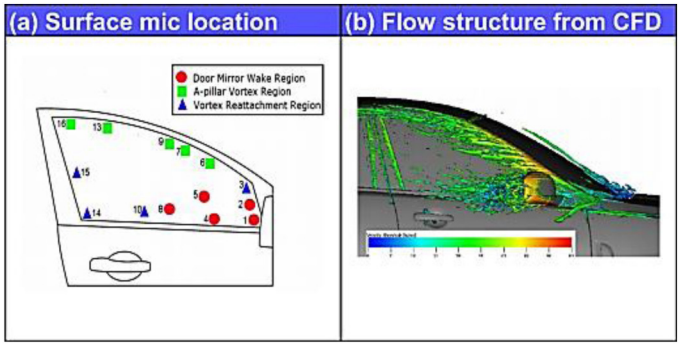

Figure 5. Schematic of driver's side-glass surface microphones (a) location and (b) flow structure[29].

Roof-Mounted Probe Measurements

To measure the onset flow, a roof-mounted multi-hole probe was used. The probe provides time-resolved measurement to O (1 kHz) of the 3 components of velocity and local stagnation and static pressure. In this case the probe was used principally to record dynamic yaw angle; the tunnel velocity reported is based on the wind tunnel bulk velocity measurement and calibration. The probe was calibrated in isolation in a dedicated probe calibration facility and the reported yaw angle is therefore the local flow at the probe.

The probe tip was positioned approximately 320 mm above the vehicle's roofline, and approximately 70 mm in front of the B-pillar. A schematic view of the probe location is shown in Figure 6. In this location both longitudinal and lateral velocities (at yaw) are exaggerated by the presence of the vehicle but the measured yaw angle remains close to the free-stream value except at the highest yaw angles. As shown in [30] this location results in a more accurate measurement of yaw angle than a probe positioned 1m in front of the vehicle stagnation point. This location over the roof also minimizes aerodynamic and aeroacoustic impact on the vehicle.

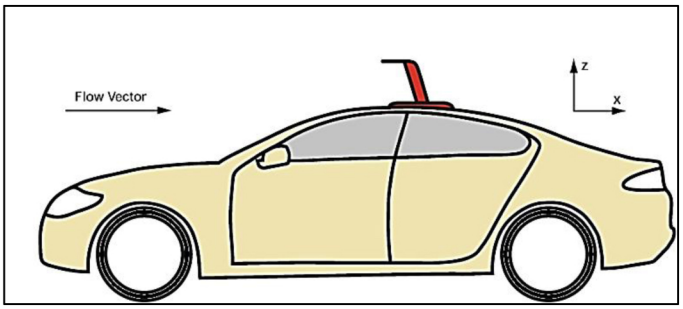

Figure 6. Test vehicle showing location of the roof mounted probe [31].

Terminology

Results are presented from instrumentation on both sides of the vehicle and consequently some care is required in order to avoid confusion on the impact of positive and negative yaw. Borrowing nautical terms, leeward and windward have been used associated with individual measurements to avoid ambiguity. The side of the vehicle that turns to face the wind is known as the windward side with the side facing away from the wind is known as the leeward side. The surface microphones were positioned on the driver's (right) side-glass of the vehicle.

As a result, under negative yaw conditions, the surface microphones and front acoustic head will be in a windward flow condition, whereas the rear acoustic head will be adjacent to the leeward side of the vehicle. This information is shown diagrammatically in Figure 7.

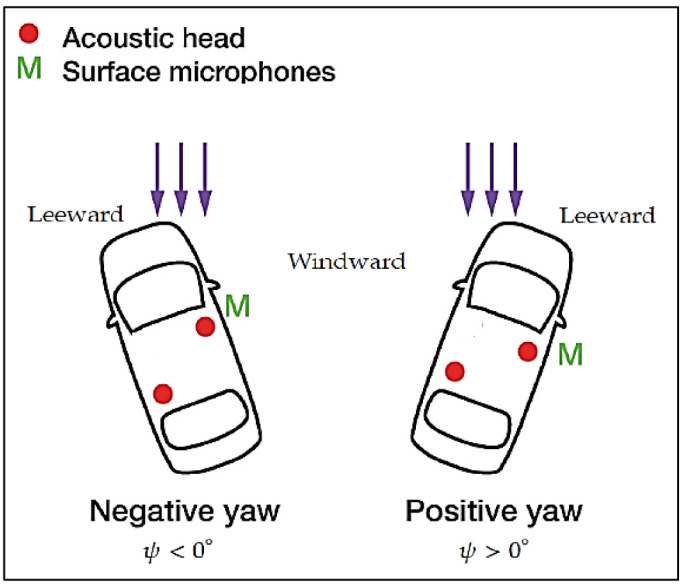

Figure 7. Location of acoustic heads and surface microphones.

Downloaded from SAE International by David Sims-Williams, Tuesday, April 21, 2015

Results - Steady State Yaw

The test vehicle was placed on the wind tunnel's turntable and rotated to different yaw angles between −10° and 10° in 5° increments. This represents the approach universally available in automotive wind tunnels. Measurements were collected using the range of techniques outlined.

Binaural Acoustic Head Measurements

The measurements presented are for a tunnel velocity of V = 130 km/h. Measurements across a range of velocities confirmed that cabin noise scaled with approximately V^6 (n = 6 dipole dominated) and with a consistent spectral make-up at all velocities.

$$\Delta SPL = 10 \log\left(\frac{U_{Res,2}}{U_{Res,1}}\right)^n \Rightarrow n = \frac{\Delta SPL}{10 \log\left(\frac{U_{Res,2}}{U_{Res,1}}\right)} \quad (1)$$

In Figure 8, the relationship between cabin noise (SPL) and yaw angle (β) is plotted for each head and ear. As expected, the outer ear (adjacent to a sideglass) always experiences a higher noise level (by 1 − 2.5 dBA) than the inner ear due to the outer ears being closer to the side-glass where the noise sources are present.

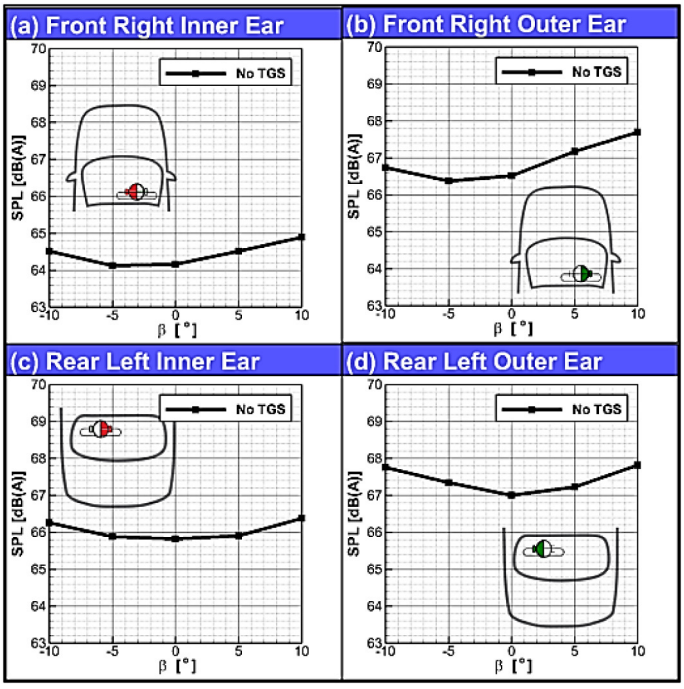

Figure 8. Overall dBA vs. β, V = 130 km/h, no TGS, for (a) FRIE, (b) FROE, (c) RLIE and (d) RLOE.

The front outer ear in particular sees elevated noise levels when its adjacent side glass is on the leeward side of the vehicle (positive yaw). The front inner ear also records higher noise levels when this head is on the leeward side.

The head on the rear seat sees a slightly higher noise level almost universally compared with the front seat head. As discussed in [23] this has been linked to underbody noise for this vehicle. Both ears on the rear head record a more symmetric variation of SPL with yaw angle compared with the front seat, indicating a more even influence from noise sources on both sides of the vehicle.

These results are all consistent with the expectation that the front sideglass (A-Pillar and mirror wake) is a key region of noise generation impacting cabin noise, particularly at leeward yaw.

Surface Microphones Measurements

SPL measurements from the microphones located on the front sideglass are presented in Figure 9. As expected, at all locations increased leeward yaw angle leads, in general, to increased surface noise level (SPL).

The microphones were sorted into classifications based on the SPL response to yaw with naming based on the location of the majority of microphones within each classification.

The microphones have been classified according to the nature of any non-linearity with yaw angle. This is because non-linearity in response to yaw has the potential to result in an impact of time-varying yaw on time-averaged SPL. A steep linear response will lead to high modulation levels, but will not affect the average whereas non-linearity leads to a time-averaged effect. The problem here is slightly more complex because SPL is not itself a linear function of the underlying acoustic pressure variation but the concept remains useful.

(a) Door Mirror Wake Region (Linear)

In the door mirror wake region (Figure 9a) the variation of SPL with yaw angle is approximately linear with a modest slope. The highest noise levels on the sideglass are seen close behind the mirror sail / stem.

(b) A-pillar Vortex Region (Sub-Linear)

The A-pillar vortex region (Figure 9b) shows high sensitivity to yaw, but with a SPL maximum before a leeward yaw of 10° is reached. This has some consistency with beamforming results, taken as part of the same investigation but not presented in this paper, where the highest SPL levels were observed at a leeward yaw angle of 5° rather than 10°.

(c) Vortex Reattachment Region (Super-Linear)

Whereas the door mirror wake region characteristic is approximately linear, and the A-pillar vortex region is sublinear (high linear term but negative quadratic term), the vortex reattachment region (Figure 9c) is characterised by an SPL vs. yaw trend which is super-linear (i.e. positive quadratic term). Mostly microphones in this region will be below the A-pillar vortex impingement/bifurcation line.

Microphone 3 was included in this region as its response with yaw is super-linear however it is obviously set apart from the other microphones in this region. It may share more in common with other microphones in this classification in terms of flow structure than is immediately obvious. Previous work [29], involved front side glass

Downloaded from SAE International by David Sims-Williams, Tuesday, April 21, 2015

surface flow visualisation on a different edition of the same vehicle and would place microphone 3 on the “Cheater reattachment line” as it was named by the authors.

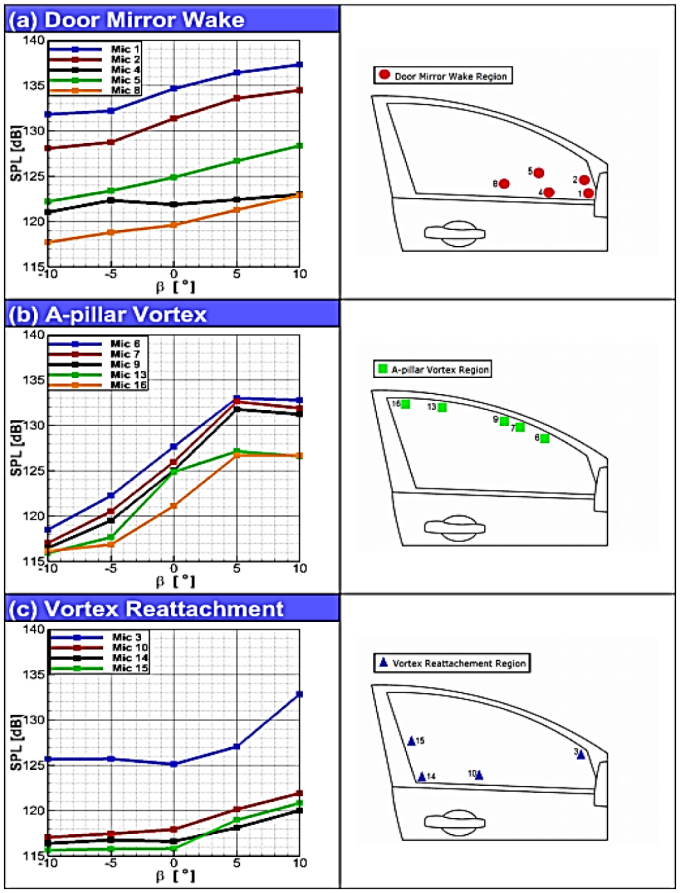

Figure 9. SPL vs. β for side-glass microphones, V = 130 km/h, no TGS.

Results - Dynamic Yaw

As introduced earlier, two different TGS modes were used, comprising a pseudo-random mode (5AL) and a dynamic yaw mode (4D1). These modes were also combined with a set of steady turntable yaw angles but much of the data presented with the TGS in operation corresponds to the turntable at zero yaw.

In addition to presenting direct measurements made with the TGS, this section also presents the results from quasi-steady analyses combining the steady-state vehicle response measured without the TGS and measured or idealised onset yaw angle distributions.

Probe Measurement of Onset Flow

The range of yaw angle experienced as a result of the TGS system has been measured using a multi-hole probe on the roof of the test vehicle. This is presented as a probability density distribution in Figure 10 along with the equivalent probe measurement without TGS. Also included is an idealized on-road probability density distribution based on roof probe measurements collected during highway driving [14]. It should be remembered that these measurements are at the probe location over the vehicle roof, where yaw variations tend to be slightly exaggerated compared with the far field and where the vehicle will introduce some unsteadiness into the flow.

It can be seen that the TGS successfully increases the range of yaw angles experienced, and that the dynamic yaw mode achieves a slightly wider yaw range than the 5AL mode.

However, a key observation is that the distribution of yaw angles as generated by the TGS is narrower than that experienced on road, with the TGS yaw angles within a range of between ±2° for the majority of the time.

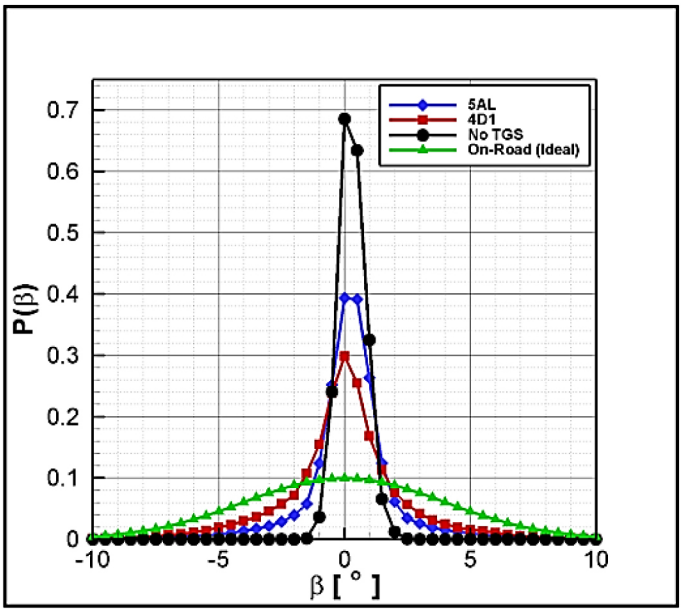

Figure 10. Yaw angle probability distributions for both TGS modes and an ideal on-road case.

Binaural Acoustic Head Measurements

Figure 11 presents in-cabin acoustic head measurements with and without TGS for a range of velocities and a range of superimposed turntable yaw angles. It is clear that the two TGS modes result in higher cabin noise than without the TGS. The two TGS modes result in a noise increment of 0.7 dBA − 0.8 dBA for both sides of the head and across all velocities and yaw angles. While only data for the head on the front seat is presented here, similar results were also noted for the rear acoustic head channels.

The increased free-stream turbulence with the TGS in operation introduces increased hydrodynamic (incompressible) pressure fluctuations as well as a small increment in acoustic background noise (compressible pressure fluctuations which propagate at the speed of sound). Both of these are essentially independent of the vehicle and so can be considered to be “background” effects, rather than part of the vehicle response to the unsteady onset flow.

The fact that the noise increment is so universal tends to suggest that it is associated with the additional background noise and increased hydrodynamic pressure fluctuations introduced by the TGS in the airflow rather than being a measure of the vehicle response to an unsteady onset flow. The third octave acoustic spectra in Figure 11c and d support this, showing that the small noise increment for the TGS modes occurs mainly within the range 30 to 70 Hz which is consistent with the in-flow turbulence fluctuations measured by the probe, The key distinction here is between the heads hearing

Downloaded from SAE International by David Sims-Williams, Tuesday, April 21, 2015

background effects (independent of the vehicle aeroacoustics) and hearing differences in the noise generated by the flow around the vehicle when the onset flow is changed.

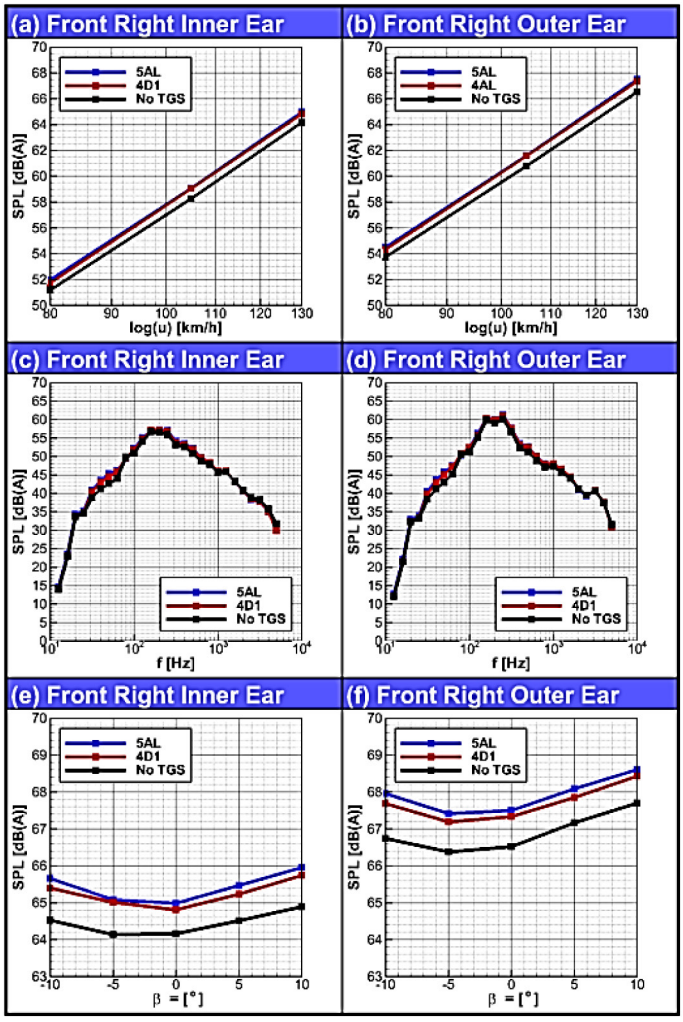

Figure 11. Overall SPL vs. velocity (a, b), frequency at 130 km/h and β = 0° (c, d) and yaw angle (e, f) with TGS modes.

Binaural Acoustic Heads Quasi-Steady Analysis

When considering an aerodynamic response to an unsteady input it is useful to begin by considering the steady state response (a quasi-steady approach). The response in the unsteady case may be below or slightly above the quasi-steady response but the quasi-steady response remains a good starting point.

Different yaw angle probability distributions (Figure 10) have been combined with the measured noise response to steady state yaw (e.g.: Figure 8) in order to predict the time-averaged noise following a quasi-steady assumption. The approach can be defined as:

$$\overline{\mathrm{SPL_{QS}}} = \sum_{\beta=-10^\circ}^{\beta=+10^\circ} \mathrm{SPL}(\beta) \cdot \mathrm{P}(\beta) \qquad (2)$$

Where SPL (β) is a direct quantification of fluctuating pressure level (e.g.: in Pa) at steady yaw angle β and P (β) is the probability of yaw angle β. When implemented this either needs to be a continuous summation (integral) or the probability defined such that the sum of all probabilities included is unity. Where SPL is presented in dB (or dBA) the integral / summation becomes:

$$\overline{\mathrm{SPL_{QS}}} = 10 \log \left[\sum_{\beta=-10^\circ}^{\beta=+10^\circ} \left(10^{\frac{\mathrm{SPL}(\beta)}{10}} \right) \cdot \mathrm{P}(\beta) \right] \qquad (3)$$

The red and green bars of Figure 12 show the result of this quasi-steady analysis applied to the steady state cabin noise response (Front Inner and Front Outer ears) combined with the measured onset yaw angles for the two TGS modes. It can be seen that the expected impact on time-averaged cabin noise is negligible (O (0.1 dBA) for either ear). This could be linked to the narrow dynamic yaw angle range achieved by the TGS.

Figure 12 also shows the actual cabin noise measurement for the TGS in operation in each mode (light blue and orange bars). Here the increment over the "No TGS" case is the universal ~0.7 dBA previously discussed. While a difference between the measurement in an unsteady environment and the quasi-steady prediction could be an indication of non-unity admittance, an admittance of O (10) is very unlikely to be physical. This supports the suggestion that the measured noise increment represents the background "self-noise" of the TGS and some propagation of turbulent hydrodynamic pressure fluctuations being transmitted into the vehicle, rather than being related to the vehicle's generation of additional aeroacoustic noise.

The small yaw angle range achieved with the TGS almost inevitably leads to a small expected impact on the time-averaged cabin noise. Hence, a yaw angle range more representative of on-road driving on a day with moderate wind is considered. Here, Equation 3 is used to combine the idealized on-road yaw angle probability density distribution from Figure 10 and the steady measured response to yaw (Figure 8).This is presented as the pink bar in Figure 12. It can be seen that, even with this wider yaw angle range the impact on time-averaged cabin noise is quite small - approximately 0.2 dBA. This result is dependent on the vehicle aeroacoustic performance at yaw. A less flat (i.e. more non-linear about β = 0°) response in Figure 8 would lead to a vehicle with a higher increment. Nevertheless, the key observation is that the impact on time-averaged cabin noise is small.

The motivation for good cabin noise performance is occupant perception. A previous study [14] collected subjective scores from a jury who listened to a range of cabin noise signals representing, among other things, vehicles with different levels of average SPL and different levels of modulation (SPL standard deviation σ). The signals were synthesized from a baseline cabin noise measurement in order to achieve both a realistic sound and a controlled parametric modification. The modulation was based on measurements of on-road onset flow unsteadiness and idealized vehicle SPL vs yaw responses. The modulation considered here is on the scale of seconds and so is below the modulation frequencies targeted by psychoacoustic measures such as "Roughness" or "Fluctuation Strength" (summarized by [32]).

Downloaded from SAE International by David Sims-Williams, Tuesday, April 21, 2015

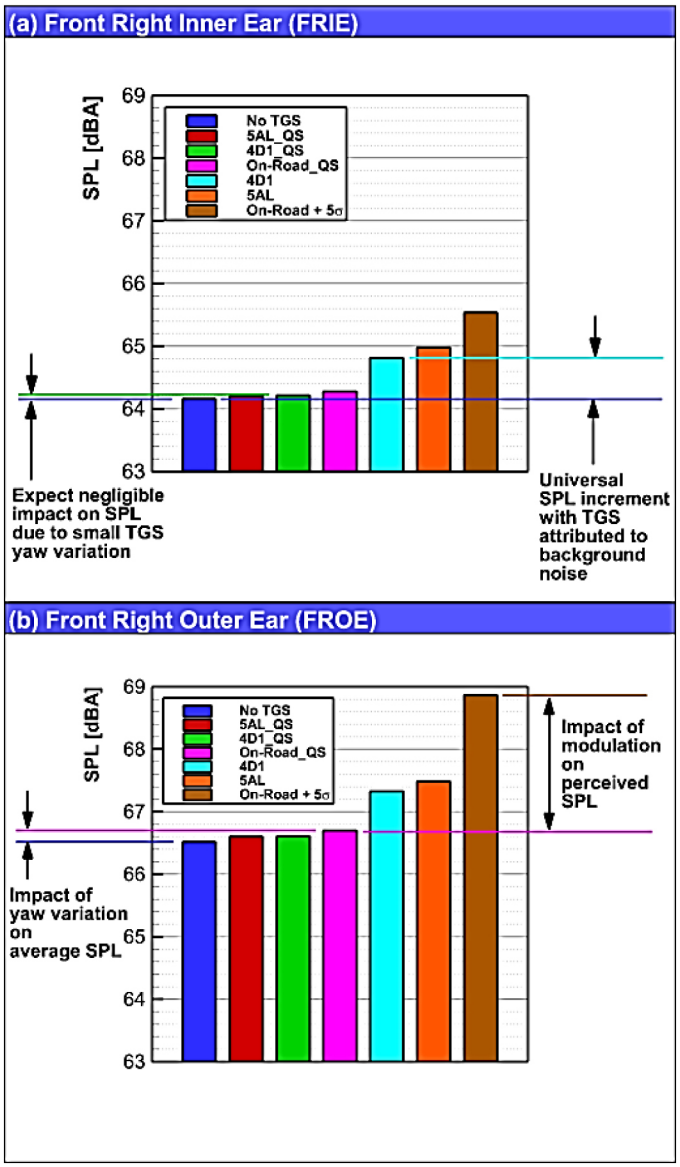

Figure 12. Overall dBA for all the test cases for (a) FRIE and (b) FROE.

The listeners effectively ranked hypothetical vehicles with different SPL at zero yaw and with different sensitivities to yaw. This jury study showed that a 1 dBA modulation (standard deviation, σ) had an impact equivalent to a 5 dBA increase in average noise level.

It is possible to approximately quantify the level of cabin noise modulation by considering the SPL standard deviation represented by the integrand in Equation 2, rather than the integral (sum). This can then be combined with the factor 5 obtained from subjective scoring in order to quantify the impact of the modulation on customer perception in terms of an equivalent increase in time-averaged cabin noise. This approach can be used to enable a better systematic ranking of designs than would be achieved by just considering the SPL measured in a wind tunnel at an isolated (e.g. zero) yaw angle.

The result for this case (using the idealized on-road yaw angle distribution) is the brown bar in Figure 12. In this case the modulation of wind noise could be expected to lead to an impact on customer perception equivalent to an increase in steady cabin noise of more than 2 dBA, This demonstrates that the modulation of cabin noise in a windy environment is much more important than the increment in time-averaged noise level, in this case 2 dBA compared with 0.2 dBA.

Correctly assessing either the time-averaged or modulation effects require a yaw angle range representative of the potential conditions on-road. Thus, achieving a large enough yaw range in a wind tunnel representation could be more significant than dynamic aspects (e.g.: frequency) of the simulation.

Side-Glass Surface Microphones

A quasi-steady analysis (as per Equation 3) was performed for the surface microphones. Figure 13 shows the measurements with and without TGS and according to a quasi-steady analysis. Results from two microphones have been selected representing interesting locations in the A-pillar vortex and vortex reattachment regions.

Surface microphones show an acute sensitivity to hydrodynamic pressure variations and the free-stream turbulence with the TGS in operation (combined with a small background noise increase) results in an increment of a few dB on the vehicle surface. However, while hydrodynamic pressure fluctuations on the vehicle surface are often strong, they tend to transmit only weakly to the vehicle interior, compared with acoustic pressure fluctuations. This is because, for any given frequency, the physical scales associated with hydrodynamic fluctuations are about an order of magnitude smaller than for acoustic fluctuations (assuming M ~ 0.1). The smaller physical scale means that hydrodynamic fluctuations do not result in a coherent loading over significant areas of the sideglass (for example) and so do not transmit effectively to the interior.

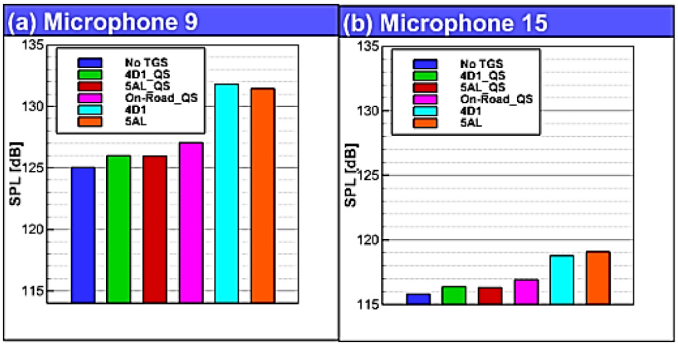

Figure 13. Overall dBA for all the test cases presented at different side-glass surface microphones placed on (a) A-pillar vortex region and (b) Vortex reattachment region

The surface microphones include a surface pressure fluctuation increment which is larger than that corresponding to a quasi-steady prediction of acoustic noise. However, this is attributed mainly to the background effect of increased turbulent hydrodynamic pressure fluctuation.

Nevertheless, it is worth observing that in selected localized regions there can be impacts from unsteadiness on the time-averaged surface noise - even if these end up lost in the overall net cabin noise. Hence differences in vehicle geometric detail or local acoustic attenuation could potentially lead to effects on time averaged cabin noise in a dynamic yaw environment.

Downloaded from SAE International by David Sims-Williams, Tuesday, April 21, 2015

Figure 14 presents surface microphone SPL varying turntable yaw combined with TGS and non-TGS cases. Microphones representing each of the three region classifications have been selected.

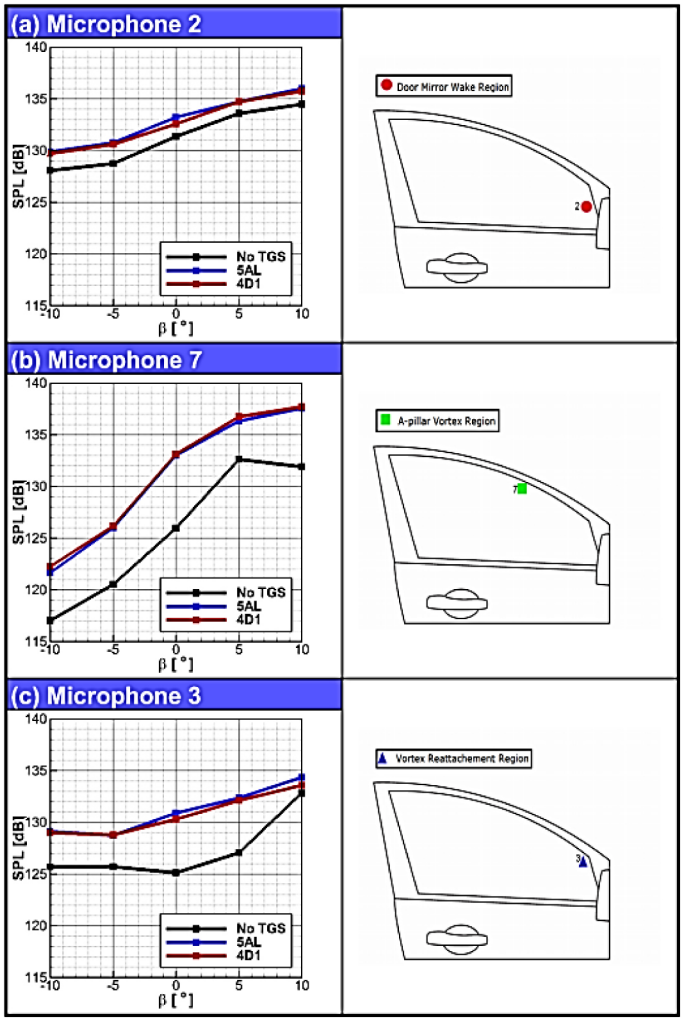

Figure 14. SPL vs. β for three side-glass microphones for both TGS modes at (a) Door mirror wake region, (b) A-pillar vortex region and (c) Vortex reattachment region at V = 130 km/h.

For the door mirror wake region the TGS modes are seen to introduce a constant noise increment across all turntable yaw angles. This is consistent with the linear steady state response of microphones in this region (Figure 9a). However, in the vortex and vortex reattachment regions the TGS increment varies with yaw angle, particularly for large leeward yaw angles. If the response were quasi-steady then the TGS modes would be expected to blur the steady state response to yaw angle and that is perhaps the case in the vortex reattachment region.

However, for the A-pillar vortex region the noise levels at leeward yaw angles seem to continue to increase in the transient situation, where they reach a maximum in the steady case. This indicates a non-quasi steady impact, perhaps the suppression of a bulk separation in the unsteady case so that the A-pillar vortex is more intense in the transient situation. This is consistent with observations in [33] of surface pressure aerodynamic admittance values greater than unity in the A-pillar region for another vehicle.

Conclusions

A vehicle driving on the road experiences unsteady flow conditions with are not generally reproduced in the development environment. This paper has investigated how this difference between the development environment and the customer's environment can influence vehicle aeroacoustics - including both the generation of noise on the vehicle exterior and the wind noise perceived by vehicle occupants. Two approaches to reproducing the effects of an unsteady wind on aeroacoustics are investigated: A Turbulence Generation System (TGS) and a quasi-steady approach based on measurements at a series of fixed yaw angles.

An important, and challenging, parameter for a wind tunnel simulation of dynamic yaw (or “Turbulence Generation System”) is achieving a wide enough variation in yaw angle. The Pininfarina TGS significantly increases turbulence levels and hence yaw angle range compared with a conventional wind tunnel and provides an important step forward, but this particular implementation does not achieve dynamic yaw angles representative of a windy on-road environment. This work indicates that capturing a representative yaw angle range is more important than reproducing the dynamics. Another challenge for wind tunnel simulation of unsteady onset flows is avoiding any artefacts that may have importance to the measured result.

An approximation of the time-varying noise generation by the vehicle can be achieved by assuming that the vehicle response at any instantaneous yaw angle is the same as it would be in the steady state (a quasi-steady approach). If the vehicle response to onset flow is non-linear then variations in onset flow will result in a difference between the time-average in an un-steady situation and a steady state case. While SPL vs. flow yaw is an example of a non-linear relationship, analysis here has shown that the expected time-averaged increment in cabin noise was less than 0.2 dBA at 130 km/h for the vehicle investigated.

This work has demonstrated that a much more important effect of time-varying onset flow is the modulation of wind noise (compared with any change to the time-averaged noise level). Using a previous assessment [14, 34] of the relative impacts of wind noise level and modulation on passenger perception this work has quantified the expected effect of time-varying onset yaw on perception. This showed that the impact of the modulation for an assumed on-road environment was equivalent to an extra 1-2 dBA in cabin noise, from the point of view of passenger perception.

While the combination of onset unsteadiness and non-linear response did not lead to important impacts on the time-averaged cabin noise, there were localized regions on the vehicle exterior where these effects had greater importance. In the A-pillar vortex region in particular the local noise levels appear to be higher than a quasi-steady approach would suggest. This seems consistent with [33] which showed similar behavior for surface pressures in this region.

References

1. Sims-Williams, D., “Cross Winds and Transients: Reality, Simulation and Effects,” *SAE Int. J. Passeng. Cars - Mech. Syst.* 4(1):172-183, 2011, doi:10.4271/2011-01-0172.

Downloaded from SAE International by David Sims-Williams, Tuesday, April 21, 2015

2. Wojciak, J., Theissen, P., Heuler, K., Indinger, T. et al., "Experimental Investigation of Unsteady Vehicle Aerodynamics under Time-Dependent Flow Conditions - Part2," SAE Technical Paper 2011-01-0164, 2011, doi:10.4271/2011-01-0164.
3. Ryan, A. and Dominy, R., "The Aerodynamic Forces Induced on a Passenger Vehicle in Response to a Transient Cross-Wind Gust at a Relative Incidence of 30°," SAE Technical Paper 980392, 1998, doi:10.4271/980392.
4. Theissen, P., Wojciak, J., Heuler, K., Demuth, R. et al., "Experimental Investigation of Unsteady Vehicle Aerodynamics under Time-Dependent Flow Conditions - Part 1," SAE Technical Paper 2011-01-0177, 2011, doi:10.4271/2011-01-0177.
5. Wagner, A. and Wiedemann, J., "Crosswind Behavior in the Driver's Perspective," SAE Technical Paper 2002-01-0086, 2002, doi:10.4271/2002-01-0086.
6. Garry, K., van Macklin, A., and Opstal, E., "*Measurement of Transient Aerodynamic Loads on Bluff Bodies at Extreme Yaw Angles*," in *Royal Aeronautical Society Vehicle Aerodynamics Conference 1994*, Loughborough, UK.
7. Kremheller, A., "*Experimental Investigation on Aerodynamic Effects During Overtaking and Passing Manoeuvres*," in *International Vehicle Aerodynamics Conference 2014*, Holywell Park, Loughborough, UK, October 14-15, 2014.
8. Schroeck, D., Krantz, W., Widdecke, N., and Wiedemann, J., "Unsteady Aerodynamic Properties of a Vehicle Model and their Effect on Driver and Vehicle under Side Wind Conditions," *SAE Int. J. Passeng. Cars - Mech. Syst*. 4(1):108-119, 2011, doi:10.4271/2011-01-0154.
9. Howell, J., "*Aerodynamic Drag in a Windy Environment*," in *International Vehicle Aerodynamics Conference 2014*, Holywell Park, Loughborough, UK, October 14-15, 2014.
10. Windsor, S., "*Real World Drag Co-Efficient - Is It Wind Averaged Drag?*," in *International Vehicle Aerodynamics Conference 2014*, Holywell Park, Loughborough, UK, October 14-15, 2014.
11. Wickern, G. and Lindener, N., "The Audi Aeroacoustic Wind Tunnel: Final Design and First Operational Experience," SAE Technical Paper 2000-01-0868, 2000, doi:10.4271/2000-01-0868.
12. Lindener, N., Miehling, H., Cogotti, A., Cogotti, F. et al., "Aeroacoustic Measurements in Turbulent Flow on the Road and in the Wind Tunnel," SAE Technical Paper 2007-01-1551, 2007, doi:10.4271/2007-01-1551.
13. Oettle, N., Sims-Williams, D., Dominy, R., Darlington, C. et al., "The Effects of Unsteady On-Road Flow Conditions on Cabin Noise: Spectral and Geometric Dependence," *SAE Int. J. Passeng. Cars - Mech. Syst*. 4(1):120-130, 2011, doi:10.4271/2011-01-0159.
14. Oettle, N., "*The Effects of Unsteady On-Road Flow Conditions on Cabin Noise*,". Ph.D. thesis, School of Engineering and Computing Sciences, Durham University, Durham, 2013.
15. Mankowski, O., "*The Wind Tunnel Simulation and Effect of Turbulent Air flow on Automotive Aerodynamics*,". Ph.D. thesis, School of Engineering and Computing Sciences, Durham University, Durham, 2013.
16. Thompson, M., Watkins, S., and Kim, J., "Wind-Tunnel and On-Road Wind Noise: Comparison and Replication," SAE Technical Paper 2013-01-1255, 2013, doi:10.4271/2013-01-1255.
17. Alam, F., Watkins, S., and Zimmer, G., "*Mean and time-varying flow measurements on the surface of a family of idealised road vehicles*,". *Experimental thermal and fluid science* 27(5):639-654, 2003, doi:10.1016/S0894-1777(02)00278-9.
18. Cogotti, A., "*Evolution of performance of an automotive wind tunnel*,". *Journal of Wind Engineering and Industrial Aerodynamics* 96(6):667-700, 2008, doi:10.1016/j.bbr.2011.03.031.
19. Duell, E., Walter, J., Yen, J., and Nagle, T., "Progress in Aeroacoustic and Climatic Wind Tunnels for Automotive Wind Noise and Acoustic Testing," *SAE Int. J. Passeng. Cars - Mech. Syst*. 6(1):448-461, 2013, doi:10.4271/2013-01-1352.
20. Murad, N., Naser, J., Alam, F., and Watkins, S., "*Computational fluid dynamics study of vehicle A-pillar aero-acoustics*,". *Applied Acoustics* 74(6):882-896,2013, doi:10.1016/j.apacoust.2012.12.011.
21. Zimmer, G., Alam F., and Watkins S.. *The Contribution of the A-pillar vortex to Passenger Car In-cabin Noise*. in *14th Australasian Fluid Mechanics Conference*. December 9-14, 2001 Adelaide University, Australia.
22. Wickern, G. and Brennberger, M., "Scaling Laws in Automotive Aeroacoustics," SAE Technical Paper 2009-01-0180, 2009, doi:10.4271/2009-01-0180.
23. Kounenis, C.D., Sims-Williams, D.B., Dominy, R.G. et al., "*Interactions between underbody aerodynamics and aeroacoustics*," in *International Vehicle Aerodynamics Conference 2014*, Holywell Park, Loughborough, UK, October 14-15, 2014.
24. Gaylard, A.P., "*Aerodynamic Development of the New Jaguar XF*,". 7th MIRA International Conference on Vehicle Aerodynamics 2008, Coventry, MIRA Ltd, Nuneaton, October 22-23, 2008.
25. Cogotti, A., "Aeroacoustics Development at Pininfarina," SAE Technical Paper 970402, 1997, doi:10.4271/970402.
26. Cogotti, A., "Upgrade of the Pininfarina Wind Tunnel - The New "13-Fan" Drive System," SAE Technical Paper 2006-01-0569, 2006, doi:10.4271/2006-01-0569.
27. Cogotti, A., "*From steady-state to unsteady aerodynamics and aeroacoustics. The evolution of the testing environment in the Pininfarina wind tunnel*,". Seventh International Symposium on Fluid Control, Measurement and Vision 2003, Sorrento, Italy, August 25-28, 2003.
28. Brüel & Kjær, "*B&K type 4949 surface microphones technical specification*,". http://www.bksv.com/Products/transducers/acoustic/microphones/microphone-preamplifier-combinations/4949?tab=overview, accessed Jan.2015.
29. Freeman, C.M., and Gaylard, A.P., "*Integrating CFD and Experiment: The Jaguar Land Rover Aeroacoustics Process*,". 7th MIRA International Conference on Vehicle Aerodynamics 2008, England, October 22-23, 2008.

Downloaded from SAE International by David Sims-Williams, Tuesday, April 21, 2015

30. Oettle, N., Mankowski, O., Sims-Williams, D., Dominy, R. et al., "Assessment of a Vehicle's Transient Aerodynamic Response," SAE Technical Paper 2012-01-0449, 2012, doi:10.4271/2012-01-0449.

31. Oettle, N., Mankowski, O., Sims-Williams, D., Dominy, R. et al., "Evaluation of the Aerodynamic and Aeroacoustic Response of a Vehicle to Transient Flow Conditions," *SAE Int. J. Passeng. Cars - Mech. Syst*. 6(1):389-402, 2013, doi:10.4271/2013-01-1250.

32. Fastl, H., and Zwicker, E., "*Psychoacoustics: Factsand models*, Third Edition,". (Springer-Verlag Berlin Heidelberg, 2007), 315-368, ISBN:978-3-642-51765-5.

33. Sims-Williams, D.B., Oettle, N.R., Mankowski, O.R., and Dominy, R.G., "*Assessment of Aerodynamic Response to Transients Through On-Road Measurements*,". IMechE Vehicle Aerodynamics Conference, 2012, Nuneaton, UK, October 30, 2012.

34. Oettle, N.R., Sims-Williams, D.B., and Dominy, R.G., "*Evaluation of the Aeroacoustic Response of a Vehicle to Transient Flow Conditions*,". FKFS - 9thAerodynamic Conference, Progress in Vehicle Aerodynamics and Thermal Management 2013, Stuttgart, Germany, October 1-2, 2013.

Contact Information

Mr. Charalampos Kounenis
Durham University, UK
Charalampos.kounenis@durham.ac.uk

Dr. David Sims-Williams
Durham University, UK
d.b.sims-williams@durham.ac.uk

Acknowledgments

The authors are grateful to Jaguar Land Rover for supporting this work and for permission to publish. Moreover, we would like to thank Dr. Mankowski and Mr. Chow as well as all the Pininfarina wind tunnel personnel for supporting the test por-tion of this work.

Definitions/Abbreviations

A_f - Frontal Area

C_d - Drag Coefficient

f - Frequency

M - Mach Number

n - Source Index

U_{Res} - Probe Resultant Velocity

V - Wind Tunnel Velocity

β - Yaw Angle

ΔSPL - Difference in Sound Pressure Levels

σ - Standard Deviation

B&K - Brüel & Kjær

CAD - Computer Aided Design

CCD - Charge Coupled Device

FRIE - Front Right Inner Ear

FROE - Front Right Outer Ear

HDM - High Definition Microphones

HMS - Head Measurement System

O( ) - Order of

P( ) - Probability of

QS - Quasi-Steady

RLIE - Rear Left Inner Ear

RLOE - Rear Left Outer Ear

SPL - Sound Pressure Level

TGS - Turbulence Generation System

The Engineering Meetings Board has approved this paper for publication. It has successfully completed SAE's peer review process under the supervision of the session organizer. The process requires a minimum of three (3) reviews by industry experts.

All rights reserved. No part of this publication may be reproduced, stored in a retrieval system, or transmitted, in any form or by any means, electronic, mechanical, photocopying, recording, or otherwise, without the prior written permission of SAE International.

Positions and opinions advanced in this paper are those of the author(s) and not necessarily those of SAE International. The author is solely responsible for the content of the paper.

ISSN 0148-7191

http://papers.sae.org/2015-01-1555